Numerical Analysis of Ion Beam Extraction Phenomena in an Ion Thruster*†

Yasushi Okawa‡
Satellite Venture Business Laboratory, Kyushu Institute of Technology
1-1, Sensuicho, Tobata, Kitakyushu, Fukuoka 804-8550, Japan
+81-93-884-3163
okawa@mech.kyutech.ac.jp

Haruki Takegahara§
Department of Aerospace Engineering, Tokyo Metropolitan Institute of Technology
6-6, Asahigaoka, Hino, Tokyo 191-0065, Japan
+81-425-85-8659
hal@astak3.tmit.ac.jp

Takeshi Tachibana¶
Department of Mechanical Engineering, Kyushu Institute of Technology
+81-93-884-3161
combust@mech.kyutech.ac.jp

IEPC-01-97

The transient beam extraction phenomenon directly after applying beam-accelerating voltage is one of the unsolved problems in an ion thruster. Although some experimental experiences concerned with this transient phenomenon have been reported, its mechanism has not been fully understood. In this study, numerical investigations were performed to explain these transient problems in ion optics with the experimental support. As a result of the preliminary experiment, it was shown that the transient phenomena could be simulated by integrating the steady state condition at each beam-accelerating voltage because the time-scale of charged particles motion was much smaller than that of voltage rising. Based on this result, the transient behavior of charged particles was calculated using a particle-in-cell simulation. The calculation results graphically explained the formation process of an ion sheath and a beamlet in transition in addition to the erosion mechanism of an accelerator grid by transient ion impingement.

---

* Presented as Paper IEPC-01-97 at the 27th International Electric Propulsion Conference, Pasadena, CA, October 15-19, 2001.

‡ Researcher, Member AIAA.

§ Professor, Senior Member AIAA.

¶ Associate Professor, Senior Member AIAA.

Introduction

Ion beam extraction from a discharge chamber plasma is one of the most important processes in an ion thruster because this process dominates thrust generation. Although a large number of studies have been made on this process, its physical phenomena have not been fully understood. One of those unsolved problems is the transient phenomenon immediately after applying beam-accelerating voltage.

At the start-up of beam extraction, large inrush current through an accelerator grid (and a decelerator grid if it exists) is usually observed in accordance with a sharp rise in beam-accelerating voltage. This passing current is thought to be caused by the direct impingement of transient diverged ions. This transient phenomenon may influence thruster design and operation in following three aspects. 1) Erosion problem. It is expected that a large number of beam on/off cycles are required to operate an ion thruster on orbits because of the influence of Earth's eclipse, the on/off operation requirements for station keeping of GEO satellites[1] and the occurrence of unexpected high-voltage breakdown (HVBD).[2][3] Such many times of beam on/off cycles result in a large number of ion impingements on grids and other spacecraft components (e.g. solar panels and antennas) in total and may cause the erosion problems. In some experiments, peculiar erosion patterns that seem to be caused by transient diverged ions have been observed on an accelerator grid surface.[4][5][6] 2) Current limit control. The magnitude of transient current through an accelerator grid in the beam start-up process is comparable to that of arcing current in a steady state operation. Hence additional current limit control is required for the beam start-up sequence independent of regular current limitation. The time-dependent profile of transient current is needed to design such a complicated circuit. 3) Cause of flakes. During the transient period discussed here, many ions impinge on the upstream surface of an accelerator grid in a very short time. Thus, the sputtered matter produced in this process may grow into flakes or peels and cause HVBD between the grids.

In order to make detailed discussion on these problems, it is important to understand the transient phenomena in ion optics and estimate the amount of ion impingement, however, little attention has been given to these points. The purpose of this study is to explain these transient phenomena of ion beam extraction directly after applying beam-accelerating voltage in an ion thruster. For this purpose, the numerical simulation code IBEX-T[7], which has been developed by the authors, was used. IBEX-T is a particle-in-cell (PIC) code that possesses the feature of full particle simulation. The influences of discharge chamber plasma properties on beam extraction performance have been investigated using this code in our previous studies.[8][9] In this study, some experiments were conducted to support the calculation results in addition to the numerical calculation.

Calculation Model

Charged particles motion is calculated in a two-dimensional axisymmetric domain with a three-dimensional velocity component for a single set of grid apertures in IBEX-T. Figure 1 depicts the computational domain with the electric potential boundary conditions. Beam extraction by two-grid system is discussed here. The calculation flow is shown in Fig. 2.

One of the features of this calculation is that both ions and electrons are treated as particles and their trajectories are followed in time. This treatment enables us to simulate the charged particles motion in plasma boundary region including the influences of non-Maxwellian electron existence in a discharge chamber plasma. Although controlled mass ratio (Electron mass is multiplied by one thousand.) is used in IBEX-T to relax

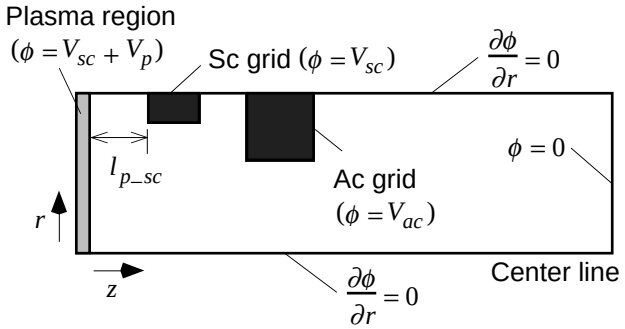

Fig. 1 Computational domain.

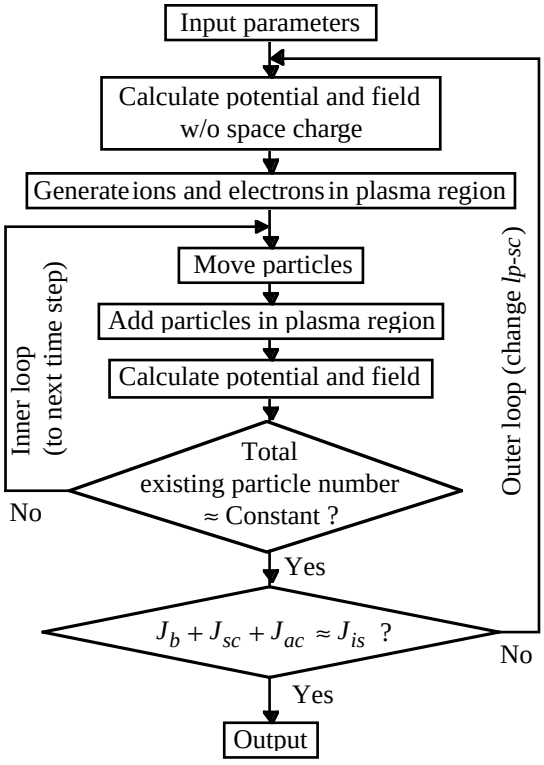

Fig. 2 Calculation flow diagram.

the severe restriction of calculation time step and mesh size, it has been confirmed that there are almost no differences between the calculation results with this controlled mass ratio and ones with physical mass ratio.[7][8]

As shown in Fig. 1, the finite region that simulates a discharge chamber plasma is placed in the upstream end of the calculation domain. In this region, the plasma properties such as number density and temperature (or energy distribution function) of ions and electrons and space potential are given optionally and kept constant throughout the calculation. If Bohm's criterion is accepted, the ion saturation current of the plasma J_{is} is obtained from the plasma properties as follows

$$J_{is} = en_{i0}\left(\frac{kT_e}{m_i}\right)^{1/2}\exp\left(-\frac{1}{2}\right)\cdot\pi R^2, \tag{1}$$

where e is elementary charge, n_{i0} is ion number density, k is Boltzmann constant, T_e is electron temperature, m_i is ion mass, and R is radial length of the calculation domain. Because the potential difference between the discharge chamber plasma and the screen grid is large enough, the equation above should be valid. In IBEX-T, this ion saturation current is used to determine the plasma-to-screen distance $l_{p\text{-}sc}$ (see Fig. 1) as shown in Fig. 2, that is, the equilibrium condition between the ion saturation current and the calculated total current

$$J_b + J_{sc} + J_{ac} \approx J_{is}, \tag{2}$$

should be satisfied to terminate the calculation. In this equation, J_b is beam current, J_{sc} is ion impingement current on a screen grid, and J_{ac} is that on an accelerator grid for a single set of apertures. Using eq. (2), ion beam extraction capability and detailed phenomena in ion optics for various discharge chamber plasma properties and ion optics condition can be calculated. This is another feature of IBEX-T.

The motion of ions and electrons is calculated in the two-dimensional axisymmetric domain with a three-dimensional velocity component (radial, axial and azimuthal). The equations of motion

$$m_i\frac{d\boldsymbol{v}_i}{dt} = e\boldsymbol{E}, \tag{3}$$

$$m_e\frac{d\boldsymbol{v}_e}{dt} = -e\boldsymbol{E}, \tag{4}$$

are solved using Euler's integration scheme. In the equations above, m_e is electron mass, $\boldsymbol{v}_i$ and $\boldsymbol{v}_e$ is ion and electron velocity respectively. Electric field $\boldsymbol{E}$ is obtained by solving Poisson's equation

$$\nabla^2\phi = -\frac{e}{\varepsilon_0}\left(n_i - n_e\right), \tag{5}$$

where ε_0 is permittivity of free space, using Gauss elimination method with sparse-matrix refinements[10] and differentiating the electric potential

$$\boldsymbol{E} = -\nabla\phi. \tag{6}$$

The calculations of the charged particles motion and the electric field are iterated in the PIC routine until the total number of existing particles in the whole calculation domain is saturated as shown in Fig. 2. The calculation is terminated after the confirmation of the current equilibrium described above.

Table 1 Input and output parameters of IBEX-T calculation.

(a) Input

Discharge chamber plasma properties	Grid geometries	Beam accelerating voltages
Ion number density, n_{i0}	Screen hole diameter, d_{sc}	Screen grid voltage, V_{sc}
Electron number density, n_{e0}	Accel. hole diameter, d_{ac}	Accel. grid voltage, V_{ac}
Ion temperature, T_i	Screen grid thickness, t_{sc}	
Electron temperature, T_e	Accel. grid thickness, t_{ac}	
Plasma space potential, V_p	Grid separation, l_g	

(b) Output

Currents for single apertures	Spatial distribution	Others
Beam current, J_b	Ion particles	Velocity distribution of beam ions
Screen ion current, J_{sc}	Electron particles	Ion sheath boundary contour
Accel. ion current, J_{ac}	Ion number density, n_i	
	Electron number density, n_e	
	Electric potential, ϕ	

In this calculation, the computational domain shown in Fig. 1 possesses the physical geometry of 1.35 mm in radial and 5.00 mm in axial and is divided to 60×250 cells. The mesh size and the time step were selected to obtain a precise and stable solution.[7][11] At present, only singly charged ions and electrons originated in the discharge chamber plasma are considered as existing particles and collisions between the particles are not taken into account. The input and output parameters of the calculation are listed in Table 1.

Experimental Setup

Transient beam current and grid impingement currents associated with a rapid increase in beam-accelerating voltage were measured using the cusped ion thruster of Tokyo Metropolitan Institute of Technology.[12] The thruster possesses the 12-cm diameter ion optics fabricated of carbon-carbon composite. The grid system consists of a screen and an accelerator grid with the following geometries: d_{sc}=2.2 mm, d_{ac}=1.3 mm, t_{sc}=0.5 mm and t_{ac}=0.5 mm. The screen-to-accelerator grid separation l_g was slightly different in radial position because of the difference of the flatness of both the grids, however, it was approximately 1.0 mm at most part of the ion optics. The properties of the discharge chamber plasma were measured using a Langmuir probe in order to use them as the input parameters of IBEX-T code.

Figure 3 shows the electric circuit for the thruster operation and the measurement of currents and voltages.

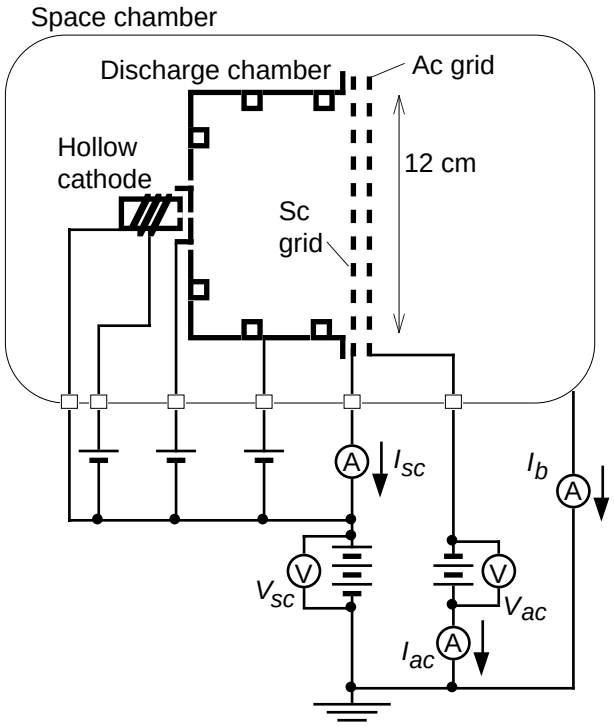

Fig. 3 Electric circuit for thruster operation and measurement.

The current from the screen grid to the high-voltage power supply was measured as the screen grid current I_{sc} in addition to the beam current I_b and the accelerator grid impingement current I_{ac}. I_{sc} can be regarded as the accumulation of J_{sc} mentioned in eq. (2) because the potential difference between the discharge chamber plasma and the screen grid is large enough to neglect the contribution of electron current. The time-dependent changes of V_{sc}, V_{ac}, I_b, I_{sc} and I_{ac} were obtained by a digitized oscilloscope.

Xenon propellant was used in the experiment and the pressure during the thruster operation was lower than 1.1×10^{-3} Pa (8.0×10^{-6} Torr) for xenon. A neutralizer cathode was not operated and an end of the chamber wall collects the ion beam as shown in Fig. 3.

Results and Discussion

Measurement of Transient Currents and Voltages

The transient behavior of beam and grid impingement currents just after applying beam-accelerating voltage was measured. The thruster operating point and typical performance in this measurement are shown in Table 2. These data were obtained in steady state (after the saturation of voltage increase). Although the thruster performance shown in Table 2 is not good compared with other state-of-the-art thrusters, it is sufficient to discuss the phenomena on ion beam extraction.

Table 2 Operating point and performance of 12-cm ion thruster.

Total propellant flow rate, $\dot{m}$, sccm	8.0
Screen grid voltage, V_{sc}, V	1000
Accelerator grid voltage, V_{ac}, V	-600
Accelerator grid current, I_{ac}, mA	5
Discharge voltage, V_d, V	32
Discharge current, I_d, A	4.0
Thrust, T, mN	22
Specific impulse, I_{sp}, s	2800
Ion production cost, C_i, W/A	310
Propellant utilization efficiency, η_u, %	71

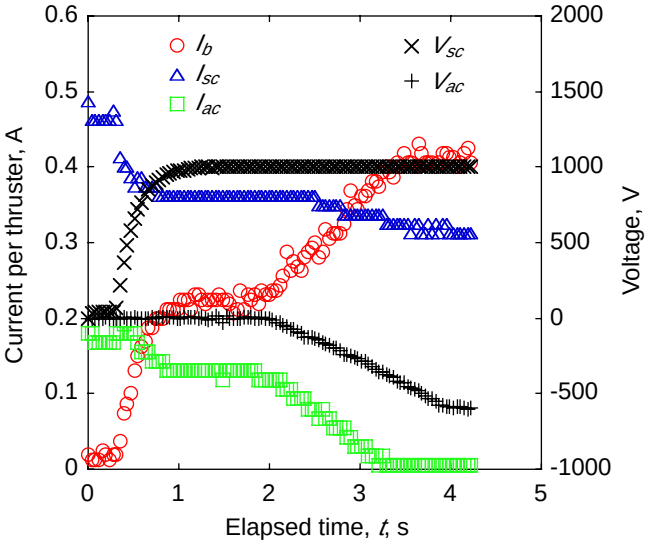

Fig. 4 Transient behavior of beam and grid currents in accordance with voltages change.

Figure 4 shows the time-dependent change of screen grid voltage V_{sc}, accelerator grid voltage V_{ac}, beam current I_b, screen grid current I_{sc} and accelerator grid current I_{ac}. In this experiment, V_{sc} and V_{ac} were applied separately to make the transient phenomena clear. The manners of the increase in V_{sc} and V_{ac} (V_{ac} is described in negative value.) depend on the characteristics of the power conditioners. Figure 4 indicates that I_b shows a simple rise with an increase in V_{sc} and V_{ac} contrary to the decrease in I_{sc} and I_{ac}. Around the point of t=3.2 s, I_{ac} becomes almost 0 ampere (approximately 5 mA in detail). This implies that the direct impingement of an ion beamlet on the accelerator grid can be neglected after this point. If we define the total accelerating voltage V_t as

$$V_t = V_{sc} + \left(-V_{ac}\right), \tag{7}$$

the time-dependent change of the voltages and currents in Fig. 4 can be redrawn as a function of V_t as shown in Fig. 5. This figure shows that how the ion saturation current of the discharge chamber plasma is divided to I_b, I_{sc} and I_{ac} as a function of V_t.

As shown in Fig. 6, I_b, I_{sc} and I_{ac} at the various conditions of V_{sc} and V_{ac} were measured in order to compare the transient current behavior illustrated in Fig. 5 with the steady state current distribution. Comparing Fig. 5 and 6, we can see that the current changes in both the figures

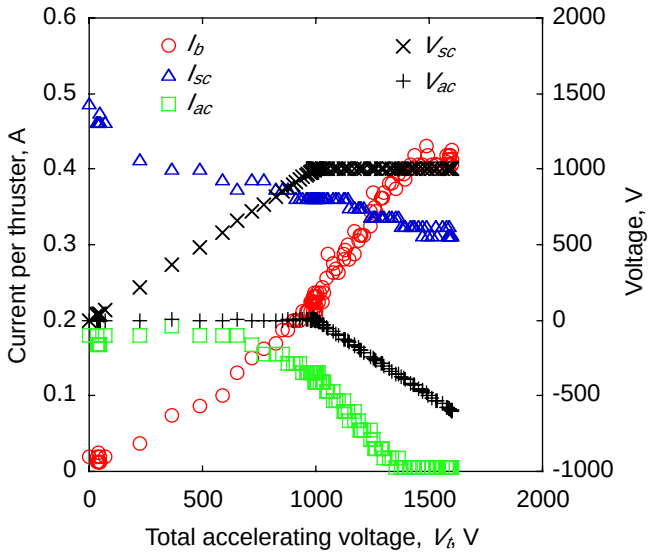

Fig. 5 Variation of beam and grid currents plotted against total accelerating voltage.

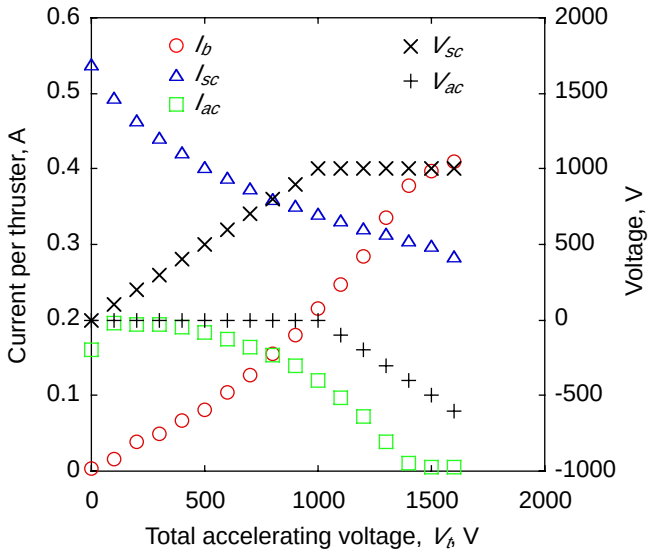

Fig. 6 Beam and grid currents vs. total accelerating voltages (steady state).

agree well with each other in qualitative and quantitative sense. I_b increases quadratically with an increase in V_t up to approximately 1400 V, then its slope becomes gentle. I_{sc} shows a simple decrease over the whole range. I_{ac} shows a slight rise adjacent to a point of V_t=0 V followed by a simple decrease up to around V_t=1400 V point. From these similarities, it is said that the transient phenomena directly after applying beam-accelerating voltage can be simulated by the accumulation of steady state phenomena at various accelerating voltages. This is because the time scale of charged particles motion is much smaller than that of the applied voltages increase. Therefore, the transient behavior of charged particles can be calculated as the integration of the steady state behavior as described below.

Calculation of Transient Currents

Based on the discussion above, beam extraction calculations were carried out at various beam-accelerating voltages to investigate the transient behavior of charged particles. As the input parameters, the discharge chamber plasma properties (listed in Table 3) at the radial position of 40 mm from the thruster axis were used as well as the grid geometries mentioned in the previous section. These plasma properties were obtained using the Langmuir probe. The ion temperature was assumed to be same as that of the discharge chamber wall. What should be noted here is that this calculation was performed for a single set of grid apertures and its results cannot be compared with experimental ones directly.

Figure 7 shows the given voltages and the calculated currents plotted against elapsed time and V_t. It was assumed that V_{sc} and V_{ac} increased separately to simulate the conditions in Fig. 4. In addition, it was also presumed that V_{sc} and V_{ac} rose linearly and it takes 1.0 second to achieve the point of V_t=1600 V (V_{sc}=1000 V, V_{ac}=-600 V) for simplicity. The reason of no plots near the V_t=0 point is that the proper results were not obtained in such a condition because of the unexpected calculation errors. Comparing Fig. 7 with Fig. 5 and 6, the variations of the beam current, screen grid current and accelerator grid current agree well between the calculation and the experiment in qualitative sense. Although we cannot

Table 3 Discharge chamber plasma properties used as imput parameters of calculation.

Radial position from thruster axis, mm	40
Axial position from ion optics, mm	30
Ion number density, n_{i0}, cm^{-3}	4.5×10^{11}
Electron number density, n_{e0}, cm^{-3}	4.5×10^{11}
Ion temperature, T_i, K	450
Electron temperature, T_e, eV	3.0
Plasma space potential, V_p, V	33

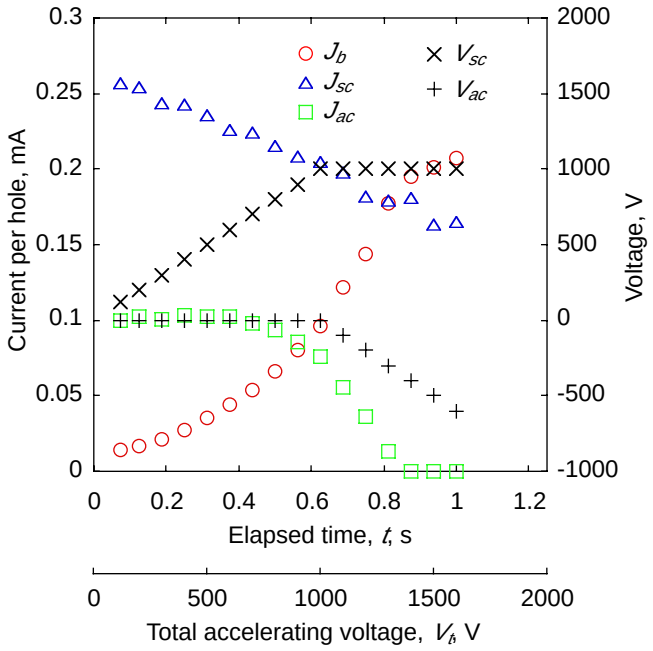

Fig. 7 Calculated beam and grid currents plotted against elapsed time and total accelerating voltage.

compare those figures quantitatively because the calculated currents are for single apertures and the measured ones are for a whole thruster, it is reasonable to say that we can discuss the transient phenomena in ion optics using IBEX-T code because the adequate qualitative validity was obtained. The normalized perveance per hole (*NP/H*) at V_t=1600 V was 1.43×10^{9} $A/V^{1.5}$.

Formation of Beamlet and Ion Sheath

The spatial distribution of ion particle, electron particle and electric potential at each elapsed time is shown in Fig. 8. In Fig. 8 (a), the state of the ion beamlet formation with an increase in time is clearly illustrated. At the beginning (lower V_t range), a distinct beamlet is not formed and greater part of ions from the plasma flow into the screen and accelerator grid. In this period, many ions impinge on the accelerator grid, however, the erosion caused by these ions is not serious because these ions do not have higher velocities. As time elapses, velocities of ions increase gradually and the converged beamlet is formed by degrees. As shown in Fig. 8 (a), quantities of ions impinge on the upstream-side surface of the accelerator grid (especially around the hole edge) in the transient period. Since the ion impingement concentrate in a short time, the sputtered matter may grow into flakes or peels that cause HVBD between the grids. Although this process has not been explained in present time, the investigation of this phenomenon should be performed as one of our future works.

It is also observed in Fig. 8 (a) that many ions that possess higher divergent angles are extracted in the transient period. Figure 9 shows the distribution of the divergence angle of the beam ions at each elapsed time. The term "divergence angle" used here denotes the angle of the velocity vector of each ion particle with reference to the hole axis. Figure 9 illustrates that the number of beam ions increases and its divergency becomes suppressed with an increase in time. In other words, at the beginning of the beam extraction process, most part of beam ions possess considerably large divergence angle though its population is not large compared with that in the steady state beam extraction. Since these divergent ions may affect on other spacecraft components such as solar panels and various antennas, they should be taken into consideration when the contamination originated in ion thrusters is discussed.

In Fig. 8 (b) and (c), it is obviously illustrated that the shape of an ion sheath near the screen grid changes from convex to concave as time passes. The fact that these detailed ion sheath formation can be described is one of the remarkable features of IBEX-T simulation .

Estimation of accelerator grid erosion caused by transient ion impingement

The estimation of the accelerator grid erosion caused by the direct impingement of diverged ions in transient period was also performed. For simplicity, the number of a beam on/off cycle was assumed to be 5000 in this estimation based on the results of our previous work on the application of an ion thruster to an orbit transfer vehicle[13] and some lifetime tests of ion thrusters.[1][4] This cycle number is thought to be reasonable for the accumulated thruster operation time of approximately 10000 hours as rough estimation. The sputtering yield of grid material (carbon-carbon composite) was assumed to be proportional to the energy of xenon ions.

Figure 10 shows the calculated erosion depth of the

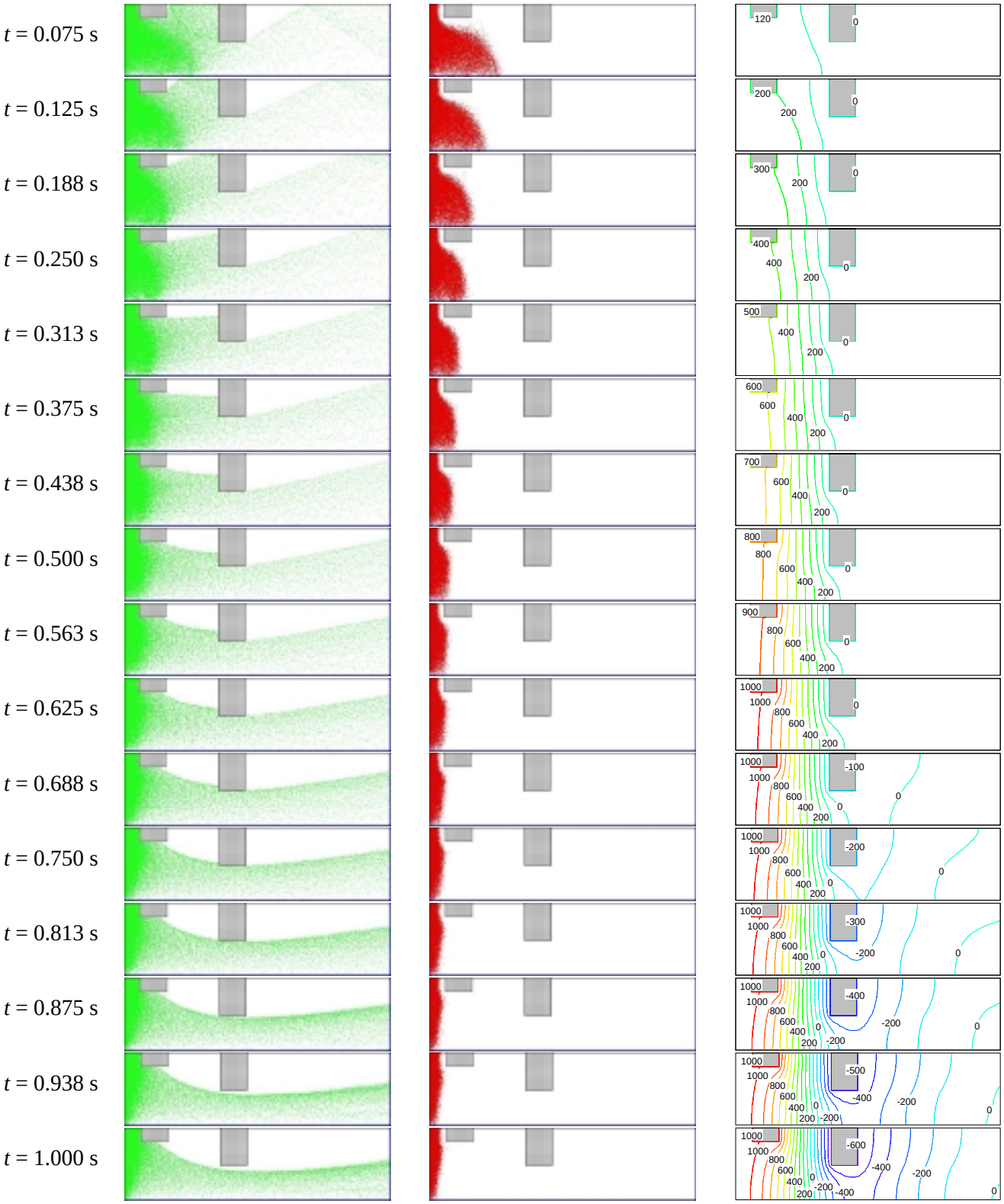

(a) Ion particle

(b) Electron particle

(c) Equipotential contours at 100 V increments

Fig. 8 Spatial distribution of ion particle, electron particle and electric potential at each elapsed time.

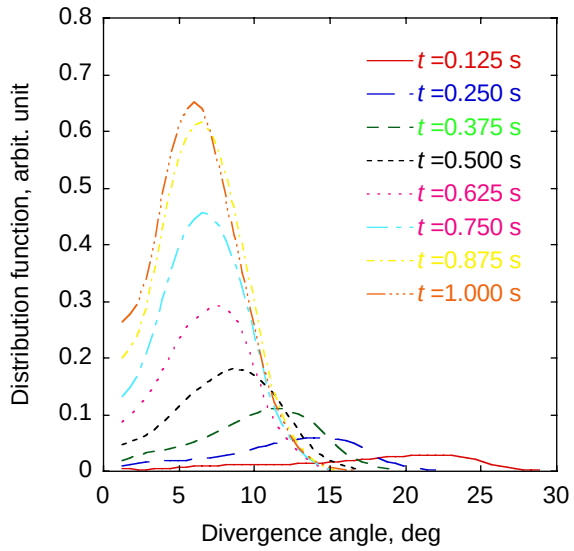

Fig. 9 Distribution of divergence angle of beam ions at each elapsed time.

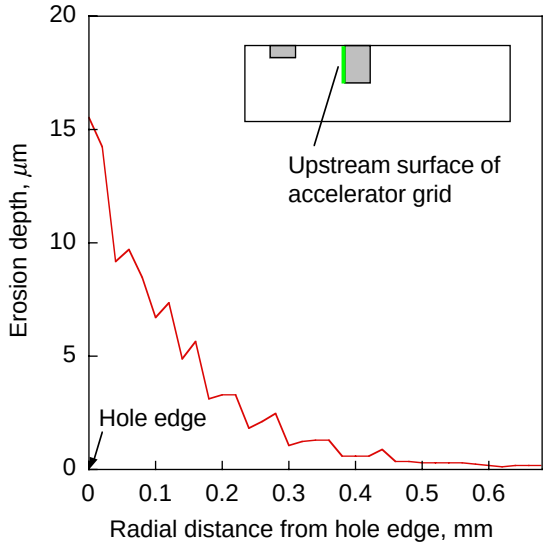

Fig. 10 Erosion depth on upstream surface of accelerator grid for 5000 beam on/off cycles. (Material: Carbon-carbon composite)

upstream surface of the accelerator grid. Although the depth is so small that it is almost negligible, the erosion pattern can be observed. In Fig. 10, it is shown that the erosion around the hole edge is extremely deep compared with that in other position and the depth decreases with increasing the radial distance from the hole edge. This erosion pattern was formed because a large number of higher-energy ions impinge around the hole edge as shown in Fig. 8. The ring shaped erosion pattern like this has been observed in some endurance tests.[4][5][6] Although these experimental results cannot be compared with our calculation result directly because the erosion pattern depends on the perveance and beam start-up sequence, it is said that this calculation can explain the mechanism of the erosion growth caused by the divergent ions in the transient time.

Table 4 Estimation of mass loss of 12-cm accelerator grid due to transient ion impingement for 5000 beam on/off cycles.

	Upstream	Inside	Total
Carbon-carbon	0.034	0.004	0.038
Molybdenum	1.51	0.19	1.70

Unit: [g]

The simple estimation of the total mass loss of the accelerator grid at the same condition in Fig. 10 is shown in Table 4. In this table, the erosion estimation for a Molybdenum grid is also listed. The figures in Table 4 are calculated by multiplying the mass loss for the single apertures by the hole quantity of the 12-cm diameter ion optics. From Table 4, it is said that the mass loss of the accelerator grid owing to the transient divergent ions is much smaller than that caused by charge exchange ions[4][5][14] if the assumption of the beam on/off rate (0.5 times an hour) mentioned above is accepted. This fact implies that the grid erosion caused by the transient ion impingement does not have serious influence on the thruster lifetime in normal operations.

Concluding Remarks

The transient phenomena of ion beam extraction immediately after applying beam-accelerating voltage in an ion thruster were investigated experimentally and numerically. In the experiment, it was shown that the transient behavior of beam current and grid impingement currents could be simulated by integrating the steady state current distribution at each beam-accelerating voltage. This is because the time-scale of charged particles motion is much smaller than that of voltage increase. Based on this result, the transient behavior of charged particles in

ion optics was calculated using a particle-in-cell code. The calculation results graphically explained the formation process of an ion sheath and a beamlet in addition to the erosion mechanism of an accelerator grid in the transient period. It was also shown that the grid erosion caused by transient ion impingement does not have serious influence on a thruster lifetime. The detailed explanation of the transient beam extraction phenomena obtained here should be useful to discuss some practical problems concerning the beam start-up process.

Acknowledgment

The authors thank Mr. Kozakai, Mr. Takeda and Mr. Hirose of Tokyo Metropolitan Institute of Technology for their experimental assistance.

References

[1] Killinger, R., Bassner, H., Kienlein, G. and Muller J., "Electric Propulsion System for Artemis," 26th IEPC, Kitakyushu, Japan, October, 1999, Vol. 1, pp. 373-380 in Proceedings (IEPC-99-054).

[2] Patterson, M. J. and Verhey, T. R., "5kW Xenon Ion Thruster Lifetest," 21st IEPC, Orlando, FL, July, 1990, (AIAA-90-2543).

[3] Hayakawa, Y., Miyazaki, K., Kitamura, S., Yoshida, H., Yamamoto, Y. and Akai, K., "Endurance Test of a 35-cm Xenon Ion Thruster," 36th Joint Propulsion Conference, Huntsville, AL, July, 2000 (AIAA-2000-3530).

[4] Shimada, S., Satoh, K., Gotoh, Y., Nishida, E., Noro, T., Takegahara, H., Nakamaru, K. and Nagano, H., "Ion Thruster Endurance Test Using Development Model Thruster for ETS-VI," 23rd IEPC, Seattle, WA, Sept., 1993 (IEPC-93-169).

[5] Toki, K., Kuninaka, H., Funaki, I., Nishiyama, K. and Shimizu, Y., "Development Status of a Microwave Ion Engine System for the MUSES-C Mission," 26th IEPC, Kitakyushu, Japan, October, 1999, Vol. 2, pp. 753-760 in Proceedings (IEPC-99-139).

[6] Hayakawa, Y., Kitamura, S., Yoshida, H., Akai, K., Yamamoto, Y. and Maeda, T., "5000-hour Endurance Test of a 35-cm Xenon Ion Thruster," 37th Joint Propulsion Conference, Salt Lake City, Utah, July, 2001 (AIAA-2001-3492).

[7] Okawa, Y. and Takegahara, H., "Numerical Study of Beam Extraction Phenomena in an Ion Thruster," *Japanese Journal of Applied Physics*, Part 1, Vol. 40, No. 1A, 2001, pp. 314-321.

[8] Okawa, Y. and Takegahara, H., "Particle Simulation on Ion Beam Extraction Phenomena in an Ion Thruster," 26th IEPC, Kitakyushu, Japan, October, 1999, Vol. 2, pp. 805-812 in Proceedings (IEPC-99-146).

[9] Okawa, Y., Satow, H. and Takegahara, H., "Investigation of Ion Beam Extraction Phenomena using a Particle Simulation Code," 22nd International Symposium on Space Technology and Science, Morioka, Japan, May-June, 2000, Vol. 1, pp. 432-437 in Proceedings (ISTS-00-b-37p).

[10] Hockney, R. W. and Eastwood, J. W., *Computer Simulation Using Particles*, Adam Hilger, Bristol, 1988, pp. 188-194.

[11] Birdsall, C. K. and Langdon, A. B., *Plasma Physics via Computer Simulation*, Inst. Phys. Publishing, Bristol, 1991, Chap. 14.

[12] Satow, H., Takegahara, H., Tachibana, T. and Kawata, K., "Application of Amorphous-Carbon Grids to an Ion Thruster," 26th IEPC, Kitakyushu, Japan, October, 1999, Vol. 2, pp. 819-824 in Proceedings (IEPC-99-148).

[13] Takegahara, H. and Okawa, Y., "Application Study of Ion Thruster to Orbit Transfer Vehicle," *Journal of the Japan Society for Aeronautical and Space Sciences*, Vol. 44, No. 508, 1996, pp. 48-55 (in Japanese).

[14] Nakano, M. and Arakawa, Y., "Ion Thruster Lifetime Estimation and Modeling Using Computer Simulation Code," 26th IEPC, Kitakyushu, Japan, October, 1999, Vol. 2, pp. 797-804 in Proceedings (IEPC-99-145).